Effect of Monomer Functionality on the Morphology and Performance of the Holographic Transmission Gratings Recorded on Polymer Dispersed Liquid Crystals

Mousumi De Sarkar,[†] Nicole L. Gill,[‡] Joe B.Whitehead,[§] and Gregory P. Crawford*[,†]

Division of Engineering, Brown University, Providence, Rhode Island 02912, and Department of Chemistry & Biochemistry and Department of Physics, University of Southern Mississippi, Hattiesburg, Mississippi 39406

Received May 13, 2002; Revised Manuscript Received November 4, 2002

ABSTRACT: Transmission gratings were formed holographically in polymer dispersed liquid crystal (HPDLC) composite materials using commercially available UV-curable acrylate monomers and the nematic liquid crystal TL203. Monomer mixtures with average functionality ranging from 1.3 to 3.5 were used to prepare HPDLC transmission gratings. The phase-separated morphology and surface topology of the transmission gratings as observed through scanning electron microscopy and atomic force microscopy varied profoundly with the different monomer mixtures characterized by their average functionalities. The switching properties of the HPDLC gratings were correlated with the morphological changes.

1. Introduction

Polymer dispersed liquid crystals (PDLCs) are extensively studied for various electrooptical applications.[1] A recent modification of PDLC is the holographically formed PDLC or HPDLC. HPDLCs are produced using holographic techniques to create a stratified composite of alternating layers of liquid crystal and polymer.[2] HPDLCs have potential application in diverse fields such as reflective flat-panel displays,[3−5] switchable lenses,[6] optical switches for telecommunication,[7] reflective strain gauge technology,[8] application-specific lenses,[9] spatially patterned devices,[10] image capture systems,[11] remote sensing,[12] and many other electrooptical applications. Since their discovery, more than 10 years ago,[13] many basic studies have been performed on the structure, morphology, and properties of HPDLCs,[14−17] and a wide variety of new configurations have evolved which include variable wavelength reflection devices,[18] multiple gratings recorded in one film,[19] polymer network versions,[20,21] devices based on smectic A liquid crystal materials, [22] formation of HPDLC based on a polarization interference pattern,[23] switchable lattices,[24] photonic crystals,[25] and formation via two-photon-induced photopolymerization.[26]

HPDLC gratings are formed by polymerization-induced anisotropic phase separation of liquid crystals from a polymer matrix created through free-radical photopolymerization.[2] Holographic imaging of laser radiation onto a homogeneous mixture of photopolymerizable monomer(s) and liquid crystal results in spatially modulated polymerization kinetics that generates alternating layers of polymer and liquid crystal rich lamellae. In general, the liquid crystal rich layers consist of randomly oriented submicrometer sized liquid crystal domains.[2] The grating morphology varies widely with the variation of LC fraction in the prepolymer syrup, intensity, and duration of irradiation and curing temperature.[2,27] Since the morphology dictates the electrooptical properties, enhanced control of liquid crystal domain size and their distribution is paramount in optimizing the overall performance of the HPDLC gratings.

The average functionality of the monomer mixture is expected to alter the phase-separated morphology and, consequently, the performance of the HPDLC gratings. The anisotropic photopolymerization and the subsequent phase separation associated with the fabrication of the HPDLC grating is a complex process. In a mixed monomer system, the reaction kinetics of the individual monomers and their contribution toward the overall polymerization process is even more complex and is thus beyond the scope of this study. Therefore, the average functionality was chosen as a parameter to characterize each of the monomer mixtures used to produce the HPDLC gratings in this study.

In recent articles the effects of monomer functionality on both reflection and transmission gratings prepared with visible radiation have been discussed.[28,29] The focus of this contribution is to establish a relationship between the average functionality and the phase-separated morphology and, therefore, the operating properties of the HPDLC transmission gratings formed with UV-initiated polymerization. In this study, different monomer functionalities were obtained using various proportions of hexa-, tri-, and monofunctional acrylates. Scanning electron microscopy (SEM) and atomic force microscopy (AFM) were used to explore the effect of monomer functionality on the morphology and the surface topology of the HPDLC transmission gratings, respectively. The polymerization kinetics of the HPDLC mixtures was investigated using a differential photocalorimeter (DPC). The electrooptic performance of the resultant HPDLC gratings was also studied.

[†] Brown University.
[‡] Department of Chemistry & Biochemistry, University of Southern Mississippi.
[§] Department of Physics, University of Southern Mississippi.
* To whom correspondence should be addressed: e-mail Gregory_Crawford@brown.edu, phone 1-401-863-2858, Fax 1-401-863-9120.

10.1021/ma020726a CCC: $25.00
Published on Web 01/08/2003

Table 1. Characteristics of Acrylated Monomers/Oligomer

monomer/ oligomer	functionality	mol wt	refractive index (20 °C)
EHA	1	184	1.436
EB4883	2	1600	1.480
TMPTA	3	296	1.474
EB8301	6	1000	1.492

2. Experimental Section

The monomer components used in this study were all commercially available acrylate derivatives. 2-Ethylhexyl acrylate (EHA) and trimethylolpropane triacrylate (abbreviated as TMPTA) were procured from Aldrich. Ebecryl 4883, a difunctional aliphatic urethane acrylate oligomer/monomer blend (abbreviated as EB4883) and Ebecryl 8301, a hexafunctional aliphatic urethane acrylate oligomer (abbreviated as EB8301), were received from UCB Radcur. In the text the oligomer EB8301 and the oligomer/monomer blend EB4883 are referred to as monomers for simplicity. Table 1 presents the functionality, molecular weight, and the refractive index values of the bulk monomers and oligomers used. The photoinitiator DAROCUR 4265 (Ciba Specialties) is a 50:50 wt % mixture of 2,4,6-trimethylbenzoyldiphenylphosphine oxide and 2-hydroxy-2-methyl-1-phenylpropan-1-one. The liquid crystal (LC) component used here was TL203, a mixture of fluorinated mesogens, procured from EM industries. The liquid crystal and monomer components were used as received from the vendors without further purification. The standard monomer mixtures contained 2 wt % of DAROCUR 4265 to initiate polymerization upon UV exposure. The components of the monomer mixtures were mixed homogeneously for 3 min in a glass vial. This isotropic syrup was then thoroughly mixed with 50 wt % of the TL203 liquid crystal. All the photopolymerizable formulations used here to prepare the HPDLC gratings comprise of fixed monomers to liquid crystal ratio of 1:1 by weight. A few drops of the monomers−LC mixture were placed between indium−tin oxide (ITO) coated glass slides separated by 5 μm glass spacers to control the thickness. The glass slides used here have an antireflection coating on the outer surfaces and an index-matching layer over the inner ITO sides. Those coatings greatly reduce the spurious reflections and waveguiding during the laser exposures that compromise the quality of the holograms.

In this study, holographic diffraction gratings were recorded by interfering two beams with a total power of 100 mW at a wavelength of 351 nm from an Ar^+ laser. After accounting for the optical losses, there was a power of approximately 22 mW in each recording beam. Typical recording time was 40 s. The holographic fringes created are normal to the substrate or parallel to the grating vector. The periodicity of the gratings was about 1 μm. HPDLC cells were then postcured for 2 min under an UV lamp to stabilize any unreacted functional groups from further photoinduced reactions.

The average functionality (F_{av}) was determined using the formula[28]

$$F_{av} = \sum \phi_i F_i \qquad (1)$$

where ϕ_i is the mass fraction of the monomer with functionality F_i .

Monomers with functionality 1, 3, and 6 were mixed to yield intermediate average functionalities. The compositions of the monomer mixtures used in this study are furnished in Table 2 along with their average functionalities. HPDLC gratings prepared with monomer mixtures with average functionalities greater than 3.5 had limited diffraction efficiencies, and HPDLC gratings made with monomer mixtures with average functionalities less than 1.3 were mechanically very weak. Therefore, the present study was limited to HPDLC transmission gratings fabricated from monomer mixtures with average functionalities ranging from 1.3 to 3.5.

A differential photocalorimeter (DPC 2920, TA instruments) was used to monitor the isothermal heat generation during the photopolymerization of the prepolymer mixtures at 30 °C under uniform UV blanket exposure. Approximately 2.6 mg of TL203/monomer mixture was micropipetted into an aluminum DSC pan with a circular divot (diameter = 3.7 mm). The filled sample pans were placed on the DPC sample head under 40 mL/min nitrogen purge and allowed to equilibrate at the cure temperature of 30 °C for 3 min. The samples were exposed for 10 min to UV light with an intensity of 40 ±3 mW/cm^2. An empty aluminum pan was used as the reference.

Table 2. Composition of Monomer Mixtures and the Corresponding Average Functionality

composition of monomer mixture			
EB8301 (wt %)	TMPTA (wt %)	EHA (wt %)	av functionality
47.5	5.0	47.5	3.5
45.0	5.8	49.2	3.4
37.8	5.4	56.8	3.0
25.0	5.0	70.0	2.4
17.8	6.0	76.2	2.0
14.7	5.3	80.0	1.8
7.4	6.5	86.1	1.5
6.0	5.9	88.1	1.4
4.6	5.1	90.3	1.3

The phase-separated morphologies of the HPDLC samples were examined with a scanning electron microscope (SEM) (JEOL 840F). The samples for SEM were prepared by freeze-fracturing the HPDLC cells using liquid nitrogen, extracting the liquid crystal using reagent-grade methanol, and then coating the exposed surface with a very thin layer of Au−Pd to minimize artifacts associated with sample charging.

Atomic force microscopy (AFM) (Nanoscope III, Digital Instrument Inc.) was employed to determine the surface topology of the transmission gratings. The HPDLC cells were disassembled and flushed with methanol several times to remove the liquid crystal in preparation for AFM analysis.

The electrooptical performance of the HPDLC gratings was determined by probing the HPDLC cells with a p-polarized He−Ne (λ = 633 nm) laser beam. A gated 1 kHz square wave voltage was applied across the HPDLC cell. The voltage amplitude was varied in consecutive experiments, and the first-order diffracted intensities were monitored. To ensure that the electrooptical properties were reasonably stable at the time of testing, all the samples were aged for 5 days prior to electrooptical characterization.

3. Results and Discussion

The polymerization kinetics of various prepolymer solutions with average functionalities ranging from 1.3 to 3.5, all containing 50 wt % of TL203 liquid crystal, was examined using a differential photocalorimeter (DPC). The heat evolved during polymerization is attributed to the reaction of the acrylated double bonds present in the monomers since LC does not participate in the photopolymerization reaction. The overall rate of polymerization is calculated from the measured heat flow using the equation[30]

$$R_p = (dH/dt)/(n\Delta H_0 m) \qquad (2)$$

where dH/dt is the heat flow taken from the DPC exotherms, n is the number of C=C bonds per monomer unit (i.e., average functionality), ΔH_0 is the standard enthalpy of the reaction for acrylate double bonds (ΔH_0 = 86.2 kJ /mol),[30] and m is the number of moles of acrylate monomers in the mixture.

The monomer conversion at a time t was calculated from the polymerization isotherm according to the equation

$$\alpha(t) = \Delta H(t)/(n\Delta H_0 m) \qquad (3)$$

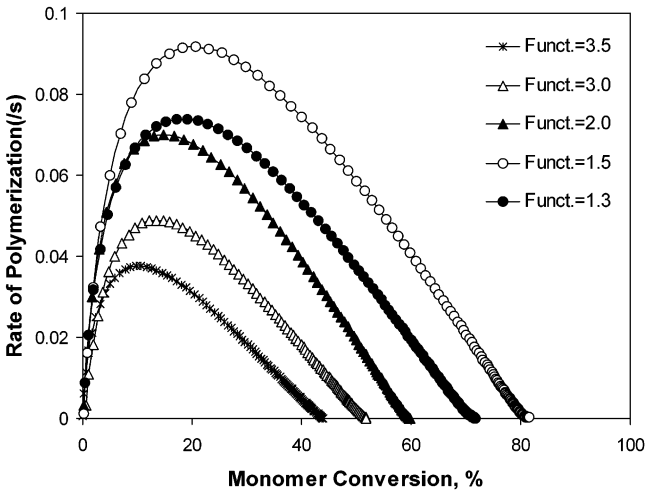

Figure 1. Rate of polymerization vs conversion of prepolymer solutions with different average functionalities.

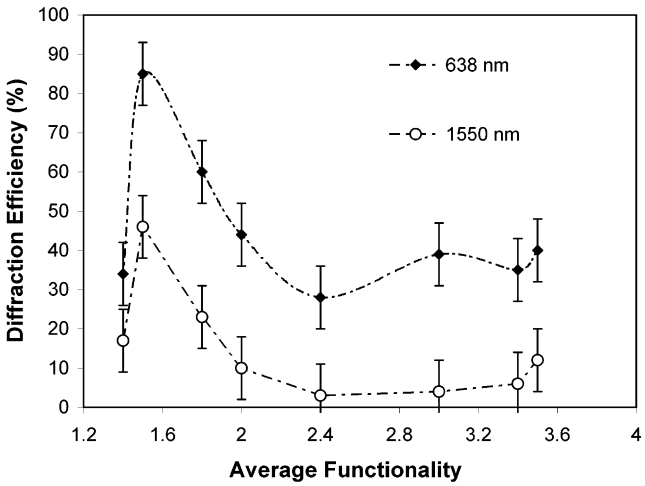

Figure 2. Average functionalities of constituent monomer mixtures against diffraction efficiency of the resultant transmission grating.

where $\Delta H(t)$ is the cumulative heat flow up to time t, n is the average functionality, ΔH_0 is the standard enthalpy of reaction for acrylate double bonds, and m is the number of moles of acrylate monomer.

The data presented here correspond to the first 4−5 min of irradiation since the extent of conversion occurring beyond this time period is insignificant. The reported data for each composition is an average of three separate photopolymerization reactions.

Figure 1 shows the rate of polymerization against the monomer conversion for mixtures with different average functionalities. There are several interesting features that are worthwhile to note. With a decrease in average functionality from 3.5 to 1.5, both the rate of polymerization and monomer conversion increase. The maximum rate of polymerization for the system with average functionality of 1.5 is more than twice as that of the system with a functionality of 3.5. The mixture with functionality of 3.5 reaches its maximum rate of polymerization at about 8% conversion whereas with average functionality of 1.5, the system attains its maximum polymerization rate at about 20% conversion. The maximum conversions for the materials with average functionalities of 3.5 and 1.5 are 44% and 82%, respectively. In general, the maximum rate of polymerization and the maximum conversion here are inversely proportional to the functionality. The exception to this trend is the mixture with an average functionality of 1.3, whose maximum rate of polymerization and extent of monomer conversion are less than the values for mixture with average functionality of 1.5 but greater than the values for average functionality of 2.0.

The inverse relationships between maximum rate of polymerization and maximum conversion with functionality are typical for acrylate monomers (refs 19 and 20 in listed ref 29). During polymerization, the probability of the reaction is proportional to the degrees of freedom of the reacting species. In principle, the higher is the mobility of the reacting species, the faster they react and the higher will be the rate of polymerization. For multifunctional acrylates, polymerization is accompanied by three-dimensional network formations. The mobility of the monomers decreases with increase in functionality as it has more reactive sites to attach with the evolving polymer network. Hence, the rate of polymerization decreases with increase in functionality. The lower final conversion for the higher functional systems could be attributed to the greater cross-linking and subsequent loss of mobility of the reactive species. However, the dependence of rate of polymerization and conversion upon functionality does not hold for the system with average functionality of 1.3. It is likely that due to the presence of large amount of monofunctional monomers (EHA > 90 wt %, Table 2), the bimolecular termination reaction becomes prevalent in that system. Moreover, since the weight fraction of each monomer components in the prepolymer formulation used here do not change monotonically, perhaps some inversion in polymerization kinetics may not be unreasonable.

Figure 2 represents the efficiency of the first order-diffracted beam with the average functionality of the HPDLC gratings for p-polarized light. It is worth mentioning here that with s-polarization all the HPDLC gratings studied here show diffraction efficiencies of only 1−2% irrespective of their different functionalities. This indicates that the orientations of the LC molecules inside the HPDLC gratings are normal to the holographic planes. The diffraction efficiency was measured at two different wavelengths: 633 nm in the visible range and 1550 nm in the IR range. Operation of the HPDLC gratings at 1550 nm is critical for their applicability in telecommunication devices. The diffraction efficiencies show similar trends at both wavelengths, although diffraction efficiencies are lower at 1550 nm as expected, since the optical thickness is reduced at longer wavelengths and the refractive index modulation also decreases with increase in wavelength.[31] The diffraction efficiencies do not change appreciably upon decreasing the average functionality from 3.5 to 2.4. The increase in diffraction efficiencies with the decrease in average functionality is much pronounced after the average functionality of 2.4. The diffraction efficiency appears to peak for average functionality of approximately 1.5 with efficiencies nearly 75% and 36% as observed with 633 and 1550 nm wavelength, respectively.

Figure 3 explores the effect of *average* functionality on the *phase-separated* morphology of the HPDLC cells. Figure 3a−e represents the SEM photographs of HPDLC cells prepared with monomers of effective functionalities of 3.5, 3.0, 2.4, 2.0, and 1.5, respectively. The liquid crystals were removed before microscopy. The

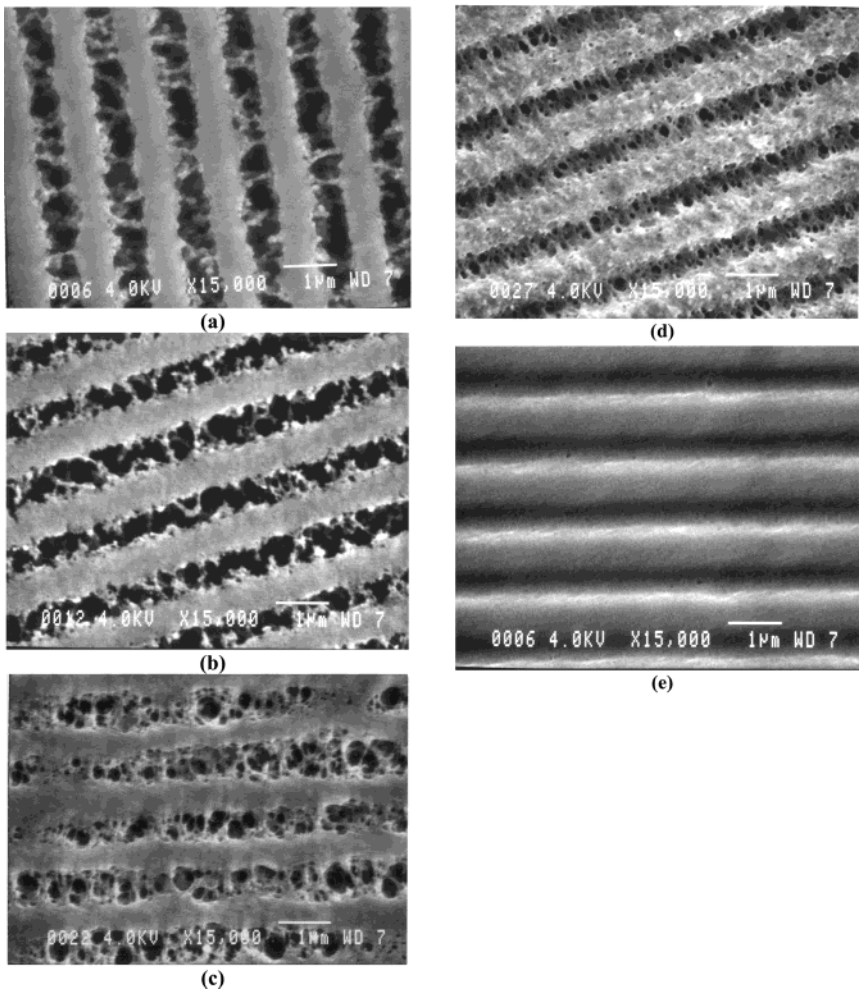

Figure 3. SEM micrographs for transmission gratings prepared using monomer mixtures with average functionalities of (a) 3.5, (b) 3.0, (c) 2.4, (d) 2.0, and (e) 1.5.

darker regions of the micrographs, revealing the absence of material, therefore, are representative of the original location of the liquid crystals. The grating microstructures with average functionalities of 3.5, 3.0, and 2.4 (Figure 3a−c) consist of spatially periodic LC crystal domains of widely distributed size separated by polymer "walls". The liquid crystal domains are more rectangular in shape with irregular edges for functionalities of 3.5 and 3.0, whereas with functionality of 2.4 (Figure 3c), the domains are more distinct and spherical in shape. Some connectivity among the LC domains is also observed. With functionality 2.0 (Figure 3d), the liquid crystal domains suddenly become much smaller, almost spherical and discrete with little disparity in their average size. For the grating with functionality 1.5 (Figure 3e), bicontinuous layers of polymer and liquid crystal have been found without any resolvable features. The LC-rich regions are devoid of any specific liquid crystal domains and resemble scaffolding morphologies. It is also interesting to note from the SEM micrographs that the ratio of the width of LC-rich regions to the polymer-rich regions decreases with decrease in average functionality. This ratio indicates the relative contributions of each of those regions in a single grating spacing. In the case of the grating with functionality 3.5, the ratio the width of LC-rich and polymer-rich regions is 0.78 (Figure 3d), whereas with functionality 2.0, the ratio is 0.45 (Figure 3a). Therefore, it can be concluded from the micrographs that the amount of phase-separated LC decreases with a decrease in average functionality of the system, which is expected because the liquid crystal is more soluble in polymer matrix formed from low-functionality monomers.

To study the effect of *average* functionality on the surface topology of the HPDLC gratings, the AFM was performed. Figure 4a−c shows the three-dimensional view of the transmission gratings formed with monomers of effective functionalities 3.5, 2.0, and 1.5, respectively, in same scale. The surfaces of all the gratings show sinusoidal-type profiles. An irregular surface relief indicating the presence of liquid crystal domains has been observed for the grating with functionality of 3.5 (Figure 4a). With average functionality of 1.5, the grating surface appears to be very smooth (Figure 4c). The grating with functionality of 2.0 shows intermediate behavior. Another interesting feature observed in AFM is that the depth of the gratings apparently increases with decrease in average functionality of the system. The average depth of grating with functionality of 3.5 has been observed through AFM to be only 0.045 μm. However, with an average functionality of 1.5, the grating depth has been seen as 0.28 μm (Figure 4c). Hence, the depth of the diffraction grating increases more than 6 times with decrease in functionality from 3.5 to 1.5. It is worth mentioning that the actual depth of the valleys of the gratings observed through AEM may be deeper than that appeared in the scan. It is possibly beyond the experimental limit of the penetra-

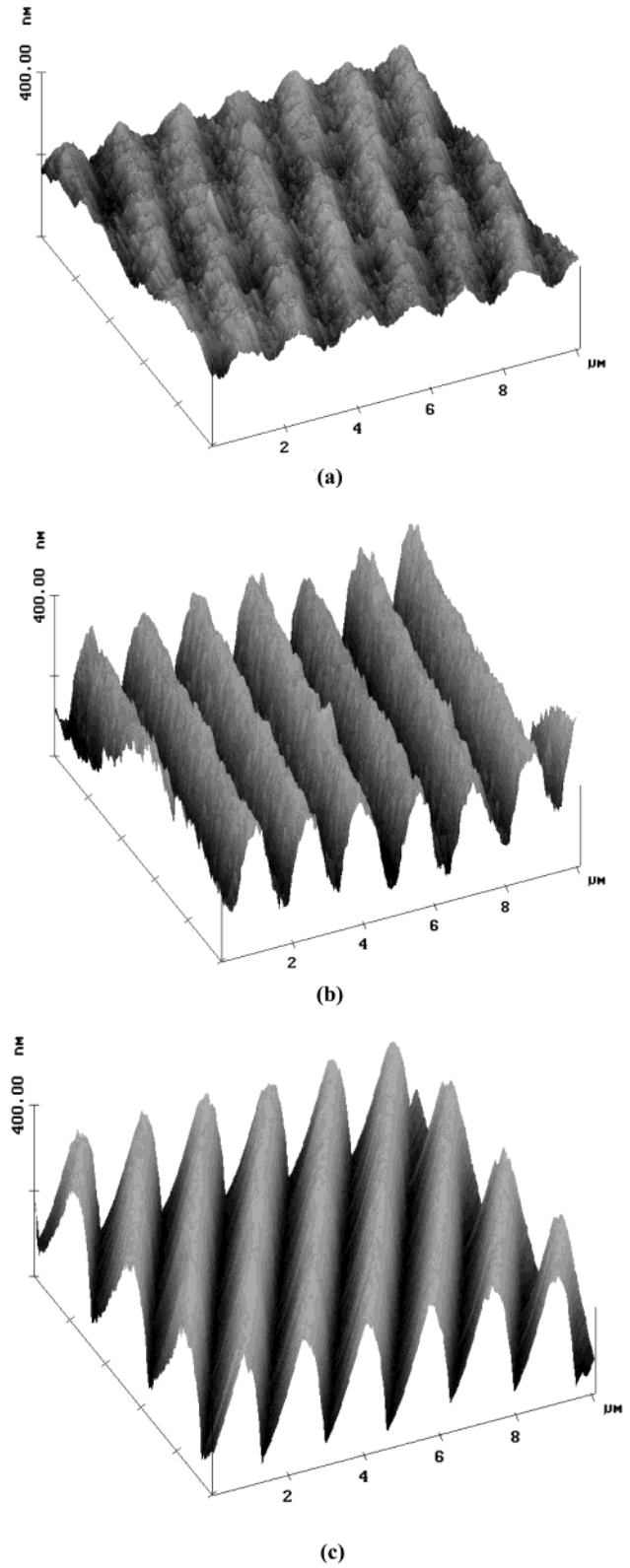

Figure 4. Atomic force microscope profiles of transmission gratings prepared using monomer mixtures of average functionalities of (a) 3.5, (b) 2.0 and (c) 1.5.

tion capacity of the pyramidal shape of the cantilever tip of the AFM.

In the hologram fabrication process, the photopolymerization preferentially initiates at the high-intensity regions. The consumption of monomer in the *high-intensity* regions gives rise to the diffusion of reactive monomers from the low-intensity regions to the high-intensity regions. On the other hand, the liquid crystal molecules diffuse to the low-intensity regions in order to equilibrate the chemical potential everywhere in the system. As the polymer network propagates outwardly from the high-intensity regions, the molecular weight of the polymer grows, even in the low-intensity regions. Eventually phase separation occurs when the LC molecules and the polymers are no longer miscible. The observations obtained from the photo-DSC measurements indicate faster *gelation* with high-functionality monomers. The strong elastic force caused by the tighter network of high-functionality systems efficiently excludes LC molecules, thereby facilitating more liquid crystals to phase separate. On the other hand, for the system with low functionality, *gelation* takes place at the later stage of the photopolymerization reaction. The phase-separated liquid crystal domains thus get little chance to expand. The weaker polymer network with low cross-link density made from low-functionality monomers incorporate more LC molecules, thereby lowering the amount of phase-separated LC. Moreover, with low-functionality monomers, the interfacial energy between the LC domains and the resulting polymer network is lower, which allows greater surface area. As a result, small and discrete nematic liquid crystal domains emerge from the system with low functionality. The SEM studies show that, with decrease in the *average* functionality of the monomers mixtures, the size of liquid crystal domains decreases. For the gratings with an average functionality 1.5 or less, no domains structures seem to be present in the LC-rich regions. The added liquid crystals are miscible at such a proportion in the loosely bound polymer network that there will hardly be any phase separation.

We observe an increase in diffraction efficiency of the transmission grating (Figure 2) and a decrease in domain size as the average functionality of the constituent monomer mixture decreases. The smaller size of LC domains can reduce the residual scattering and therefore increase the diffraction efficiency. The increase in diffraction efficiency with decrease in functionality can also be attributed to the increase in refractive index modulation.

During the formation of gratings, the rate of anisotropic diffusion of monomers toward the high-intensity illumination region is inversely proportional to their functionality. It is reasonable to assume that, at any instance during polymerization process, the concentration of monofunctional monomers would be higher in the high-intensity regions. On the other hand, the multifunctional monomers with more cross-link sites get attached with growing polymer chains fairly easily, and their movements thereby become restricted. The higher-functionality monomers thus cannot diffuse readily out of the low-intensity regions. As a result, the extent of diffusion toward high-intensity regions is much less with higher-functionality monomers compared to that of low-functionality monomers. Since the prepolymer syrups used here contain both mono- and multifunctional monomers, a significant modulation of cross-link density across the grating is created. The modulation of cross-link density is expected to be more significant for the prepolymer syrups with lower average functionality as they contain much higher proportions of monofunctional monomers (Table 2). The AFM observation of higher depth of grating grooves fortifies the assumption of larger difference between the cross-link densities

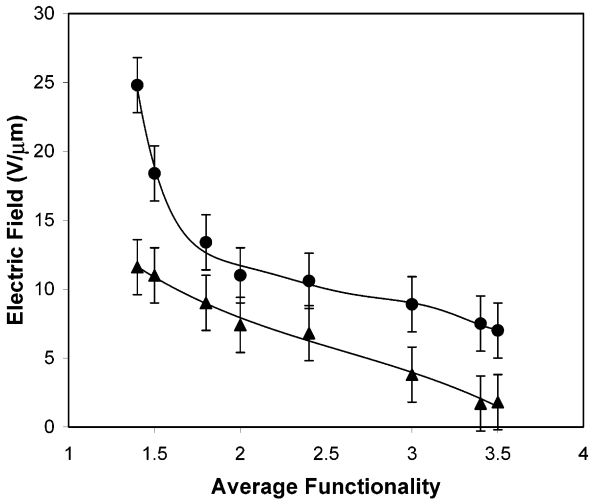

Figure 5. Influence of average functionality of constituent monomers on the electrooptical properties of transmission gratings. Smooth lines are superimposed through the experimental points to show the trends.

between high- and low-intensity regions of the grating made from low-functionality monomers.

Figure 5 shows the effect of the average functionality on the performances of the gratings in response to the applied electrical field. E_{90} and E_{10} are defined here as the electric fields required to attain 90% and 10% of its zero field efficiency of the first-order diffraction peak. It has been observed that E_{90} almost steadily increases with decrease in functionality. The E_{10} increases slightly with decrease in average functionality from 3.5 to 2.0. With further decrease in functionality from 2.0, a sudden increase has been observed in E_{10}. Switching performance of HPDLC cell, in general, diminishes as the size and distribution of nematic domains decrease. Both E_{90} and E_{10} observed in the present study decrease with increase in functionality of the constituent monomer mixtures. It has been observed through SEM that the size of the LC domains increases with increasing average functionality. In the electrooptical measurements, it has been seen that the E_{10} values also decrease rapidly with average functionality over 2.0. This observation strengthens the conclusion that E_{10} particularly is dependent on the domain size.

To examine the effect of functionality of the individual monomers on the behavior of the resulting HPDLC cells, two gratings of same average functionality of 1.5 were prepared by taking two different combinations of monomers. One of the gratings was made with difunctional acrylate (EB4883) and monofunctional acrylate (EHA). Another grating was prepared from the prepolymer syrup consisting hexafunctional acrylate (EB8301) and monofunctional acrylate (EHA). The compositions of the two monomer mixtures are shown in Table 3.

Figure 6 demonstrates the polymerization kinetics as observed through photo-DSC for two above-mentioned prepolymer mixtures with identical functionality. Both the mixtures include 50 wt % of TL203 liquid crystal. Despite possessing the same functionality, the rate of polymerization is higher for the prepolymer syrup consisting of di- and monofunctional acrylates. The maximum conversion is not significantly different for these two monomer mixtures.

SEM micrographs for HPDLC gratings from these mixtures show similar channel-like structure without any indication of nematic domains. These SEM micrographs do not have enough resolutions to differentiate among their morphologies precisely and hence are not presented here. However, there is a striking resemblance observed in the morphologies of all gratings prepared from monomer mixtures of overall functionality of 1.5 regardless of the functionality of the individual constituting monomers. The liquid crystal domains, if at all present in those gratings, are far too small to be visualized clearly through SEM (as shown previously in Figure 3c).

Table 3. Composition of Monomer Mixtures with Identical Functionality and Glass Transition Temperatures of the Corresponding Polymers

monomer composition (wt %)	mixture A	mixture B
EHA (monofunctional)	89.6	51.1
EB8301 (hexafunctional)	10.4	0
EB4883 (difunctional)	0	48.9
glass transition temp (T_g),[a] °C	−40	1

[a] The glass transition temperature of the polymers made from mixtures A and B were determined by DMA measurements at a heating rate of 10 °C/min with a frequency of 1 Hz. The T_g corresponds to the peak in loss modulus.

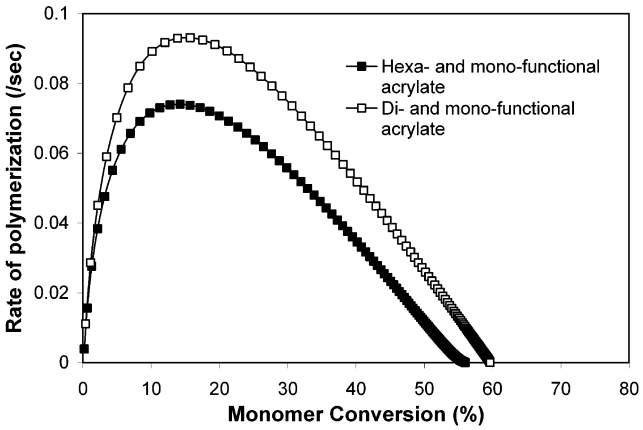

Figure 6. Rate of polymerization vs conversion of prepolymer solutions with identical average functionalities.

Figure 7a,b depicts the surface topology of the HPDLC cells with same average functionality of 1.5 as observed through AFM studies. Despite possessing identical average functionality, the surface topologies of the gratings are notably different though the SEM studies showed comparable morphologies. The irregularities observed in the two-dimensional surface profile plot for the grating consist of hexa- and monofunctional monomers may indicate the presence of the domains in it (Figure 8a). On the other hand, the profile for the grating prepared with di- and monofunctional monomers is much regular and devoid of any sort of roughness on the surface. The depth of the grating prepared with di- and monofunctional monomers (Figure 7b) is much more compared to that prepared with hexa- and monofunctional monomers (Figure 7a). The surface profile for HPDLC cell composed of di- and monofunctional monomers (Figure 7b) shows blunt peaks. Most probably the depth of the gratings is so much that the AFM tip cannot enter fully though it. The blunt shape of the peak may be attributed to the weak nature of the network. The AFM tip may cause a slight deformation of the top surface of the grating during measurements.

The functionality of the individual monomer units defines the microstructural characteristics of the resultant polymer. Despite being prepared from two monomer mixtures with identical average functionality, the in-

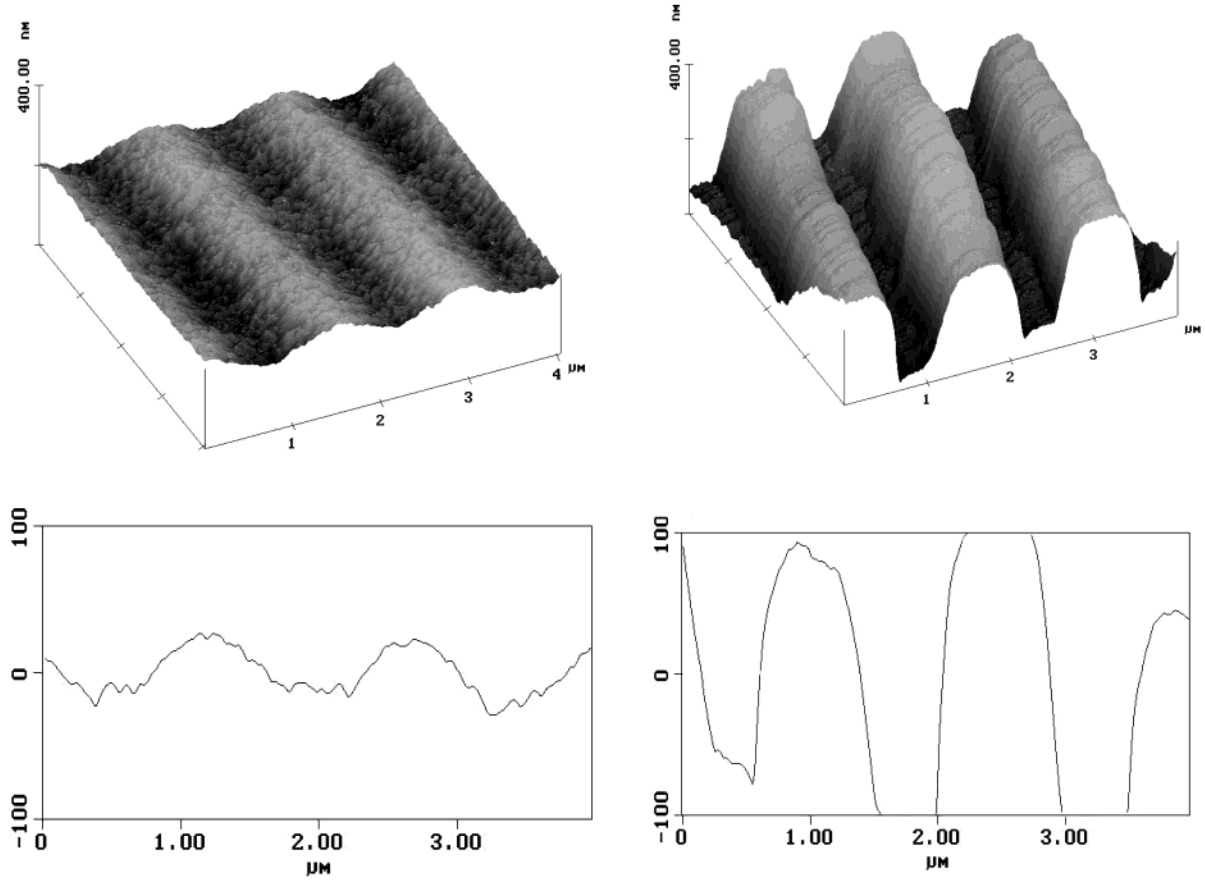

Figure 7. Atomic force microscope profiles of transmission gratings prepared from (a) hexa- and monofunctional acrylates and (b) di- and monofunctional acrylate.

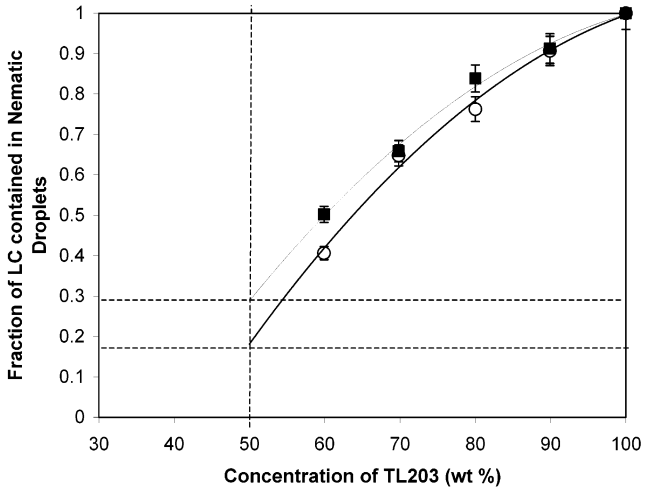

Figure 8. Fraction of LC contained in nematic droplets in PDLC made from mixtures containing hexa- and monofunctional acrylates and di- and monofunctional acrylate.

herent properties of the ensuing polymer matrices are widely different. The glass transition temperatures of the polymers obtained from those two different monomer combinations (mixtures A and B) are shown in Table 3. The higher glass transition temperature for the polymer with di- and monofunctional monomers is indicative of presence of tighter and more homogeneous cross-links compared to that made with hexa- and monofunctional monomers. The difference in cross-link density between the two polymers is attributed to the difference in molecular architecture and the reactivity ratios of the constituent monomers. Because of the presence of higher proportion of monofunctional monomer and widely different reactivity among the constituent monomers in mixture A (Table 3), the resultant polymer is very weak mechanically, which is reflected in its very low glass transition temperature.

Performance of the HPDLC gratings depends largely on the volume fraction of the phase-separated LCs as well as on their size and distributions. Since the morphology of the HPDLC gratings prepared from mixtures A and B failed to give any information about the extent of phase separation of the liquid crystal from the polymer matrix, a measure was taken to estimate it indirectly from the calorimetric studies of PDLC films made from those two mixtures using identical conditions. The PDLC samples were made inside the DSC sample pans with different LC loadings ranging from 40% to 90%. The relative amount of LC (δ) in the nematic LC domains present in PDLC samples can be determined directly through the DSC data using the following equation:[32]

$$\delta = (100/x)(\Delta H_{NI}(x)/\Delta H_{NI}(\mathrm{LC})) \qquad (4)$$

where $\Delta H_{NI}(x)$ and $\Delta H_{NI}(\mathrm{LC})$ are the enthalpy changes at nematic−isotropic transitions observed in PDLC containing x wt % LC and in the pure liquid crystal, respectively.

Figure 8 illustrates the dependence of δ on the concentration of LC for two PDLC systems with identical functionality. The trend lines between the experimental data points are extrapolated to 50 wt % of

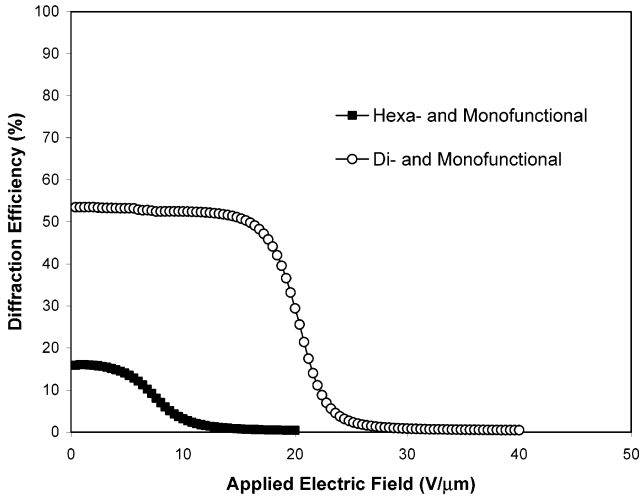

Figure 9. Diffraction of transmission gratings with applied electric field. The transmission gratings possess identical average functionality but made with different monomer combinations.

TL203. (Note that 50 wt % of the LCs were used throughout this article for the preparation of HPDLC cells.) With 50 wt % of LC loading, it was not possible to determine ΔH_{NI} precisely for PDLC as the nematic-to-isotropic phase transition peak observed through DSC became negligibly weak. It has been observed that, with 50 wt % TL203 added, only around 17 ± 2% of it will phase separate for the system with hexa- and monofunctional monomer whereas with di- and monofunctional monomers around 29 ± 2% of the added liquid crystal will phase separate. The remaining amount of added liquid crystals is plasticized in the matrix. It is evident from Figure 8 that more liquid crystals separate out from the polymer matrix made from mixtures consisting of di- and monofunctional monomers. It is worth mentioning here that the phase separation processes occurring in PDLC and HPDLC are fundamentally different as in the PDLC the process is isotropic, whereas in HPDLC it is anisotropic. Hence, the volume fraction of LC phase-separated out from the polymer matrix in the PDLC systems will not be quantitatively the same as that from HPDLCs. However, it is expected that the difference in the amount of phase-separated LCs observed in PDLC systems will sustain, at least qualitatively, in HPDLCs prepared from two monomer mixtures with same functionality.

Figure 9 compares the effect of type of monomers on the overall electrooptical performances of the HPDLC gratings. The diffraction efficiency values, as observed using $\lambda = 633$ nm probe, are plotted against the applied electrical field for the two above-mentioned gratings with identical functionality of 1.5. It has been observed (see Figure 9) that the HPDLC grating prepared with hexa- and monofunctional monomers has lower diffraction efficiency and lower switching voltages compared to the HPDLC grating prepared with di- and monofunctional acrylates. The diffraction efficiencies observed for HPDLC gratings made from hexa- and monofunctional monomers and di- and monofunctional monomers are 16% and 53%, respectively. The E_{90} and E_{10} values for HPDLC gratings prepared with hexa- and monoacrylates are 7.0 and 10.0 V/μm, respectively, whereas the grating made from di- and monofunctional monomer shows E_{90} and E_{10} as 15.8 and 23.4 V/μm, respectively. The higher diffraction efficiency observed for the gratings prepared from di- and monofunctional monomer may be attributed to the better phase separation of the LC from the polymer matrix. However, the higher volume fraction of the phase-separated LCs does not account for the higher switching voltages required for the grating with di- and monofunctional monomers. The AFM data indicate the presence of LC domains in the grating with hexa- and monofunctional monomers. It is worth mentioning that the small difference in the domain size alone cannot account for the significant difference in the switching voltages between the HPDLC gratings with identical functionality since the nematic domains present in the HPDLC gratings made with hexa- and monofunctional monomers are fairly small, and their presence has been indicated only through AFM but not with SEM.

The anchoring energy between the polymer scaffolding and liquid crystal can play a key role in determining the electrooptical performance of the gratings. As the properties of polymer matrices obtained from the two monomer mixtures (A and B) are radically different, it is expected that they would also demonstrate different anchoring energies which may result in difference in electrooptical performance of HPDLC cells. The quantitative estimation of the anchoring energies of those two systems is beyond the scope of this article.

Much more fundamental work is needed to determine the actual cause behind the radically different electrooptical performance of those two gratings. Nevertheless, the results obtained so far show that the average functionality of monomer mixture influences the performance of the ensuing HPDLC gratings.

4. Conclusions

The present study has revealed a definite connection between average functionality of the constituent monomers on the morphology and performance of the HPDLC transmission gratings formed with UV radiation. Observations through scanning electron microscopy (SEM) and atomic force microscopy (AFM) indicate a decrease in nematic domain size in the grating morphology with decrease in average functionality of the prepolymer syrup. HPDLC cells prepared from monomer mixtures with higher average functionality exhibit more variability in the shape and size of the LC domains. An optimum average functionality ($F_{eff} \approx 2.0-2.5$) exists below which the LC domains become negligibly small. The switching performance of the HPDLC gratings deteriorates with decrease in functionality showing a definite dependency of electrooptical characteristics on the grating morphology.

Acknowledgment. The authors acknowledge NASA (NAG8-1684), and G.P.C acknowledges the National Science Foundation (DMR-9875427).

References and Notes

(1) Drazaic P. S. *Liquid Crystal Dispersions*; World Scientific: Singapore, 1995.
(2) Bunning, T. J.; Natarajan, L. V.; Tondiglia, V. P.; Sutherland, R. L. *Annu. Rev. Mater. Sci.* **2000**, *30*, 83.
(3) Tanaka, K.; Kato, K.; Date, M.; Sakai, S. *SID Digest Technol. Pap.* **1995**, *26*, 267.
(4) Crawford, G. P.; Fiske, T. G.; Silverstein, L. D. *SID Digest Technol. Pap.* **1996**, *27*, 99.
(5) Bunning, T. J.; Natarajan, L. V.; Sutherland, R. L.; Tondiglia, V. P. *SID Digest Technol. Pap.* **2000**, *31*, 121.

(6) Domash, L. H.; Chen, Y.-M.; Gomatam, B. N.; Gozewski, C. M.; Sutherland, R. L.; Natarajan, L. V.; Tondiglia, V. P.; Bunning, T. J.; Adams, W. W. *Proc. SPIE* **1996**, *2689*, 188.
(7) Domash, L. H.; Chen, Y.-M.; Gozewski, C.; Haugsjaa, P.; Oren, M. *Proc. SPIE* **1997**, *3010*, 214.
(8) Cairns, D. R.; Bowley, C. C.; Danworaphong, S.; Fontecchio, A. K.; Crawford, G. P.; Li, L.; Faris, S. M. *Appl. Phys. Lett.* **2000**, *77*, 2677.
(9) Popovich, M.; Sagan, S. *SID Digest Technol. Pap.* **2000**, *31*, 1060.
(10) Fontecchio, A. K.; Escuti, M. J.; Bowley, C. C.; Sethumadhavan, B.; Crawford, G. P.; Li, L.; Faris, S. *SID Digest Technol. Pap.* **2000**, *31*, 774.
(11) Fiske, T. G.; Silverstein, L. D.; Colegrove, J.; Yuan, H. *SID Digest Technol. Pap.* **2000**, *31*, 1134.
(12) Fontecchio, A. K.; Bowley, C. C.; Crawford, G. P. *Proc. SPIE* **1999**, *3800*, 36.
(13) Margerum, J. D.; Lackner, A. M.; Ramos, E.; Smith, G. W.; Vaz, N. A.; Kohler, J. L.; Allison, C. R. US Patent No. 4,938,568, 1990.
(14) Bharadwaj, R. K.; Bunning, T. J.; Farmer, B. L. *Liq. Cryst.* **2000**, *27*, 591.
(15) Jazbinsek, M.; Olenik, I. D.; Zgonik, M.; Fontecchio, A. K.; Crawford, G. P. *J. Appl. Phys.* **2001**, *90*, 3831.
(16) Vaia, R. A.; Tomlin, D. W.; Schulte, M. D.; Bunning, T. J. *Polymer* **2001**, *42*, 1055.
(17) Kyu, T.; Nwabunma, D.; Chiu, H.-W. *Phys. Rev. E* **2001**, *63*, 061802.
(18) Bowley, C. C.; Kossyrev, P. A.; Crawford, G. P.; Faris, S. *Appl. Phys. Lett.* **2001**, *79*, 9.
(19) Bowley, C. C.; Fontecchio, A. K.; Crawford, G. P.; Lin, J.-J.; Li, L.; Faris, S. *Appl. Phys. Lett.* **2000**, *76*, 523.
(20) Silverstein, L. D.; Fiske, T. G.; Crawford, G. P. US Patent No. 6,133,971, 2000.
(21) Kato, K.; Hisaki, T.; Date, M. *Jpn. J. Appl. Phys.* **1999**, *38*, 1466.
(22) Date, M.; Takeuch, Y.; Kato, K. *J. Phys. D***1999**, *32*, 3164.
(23) Cipparrone, G.; Mazzulla, A.; Russo, G. *Appl. Phys. Lett.* **2001**, *78*, 1186.
(24) Escuti, M. J.; Crawford, G. P *SID* **2002**, *33*, P-20.
(25) Tondiglia, V. P.; Natarajan, L. V.; Sutherland, R. L.; Tomlin, D.; Bunning, T. J. *Adv. Mater.* **2002**, *14*, 187.
(26) Bunning, T. J.; Kirkpatrick, S. M.; Natarajan, L. V.; Tondiglia, V. P.; Tomlin, D. W. *Chem. Mater.* **2000**, *12*, 2842.
(27) Crawford, G. P.; Zumer, S. *Liquid Crystals in Confined Geometries formed by Porous and Polymer Networks*, 1st ed.; Taylor and Francis: London, 1996.
(28) Fontecchio, A. K.; Bowley, C. C.; Yuan, H.; Crawford, G. P. *Mol. Cryst. Liq. Cryst.* **2000** *352*, 399.
(29) Bunning, T. J.; Natarajan, L. V.; Tondiglia, V. P.; Dougherty, G.; Southerland, R. L. *J. Polym. Sci., Part B: Polym. Phys.* **1997**, *35*, 2825.
(30) Brady, G. A.; Halloran, J. W. *J. Mater. Sci.* **1998**, *33*, 4551.
(31) Moore, J. E. *UV Curing Sci. Technol.* **1978**, *1*, 133.
(32) Hariharan, P. *Optical Holography*; Cambridge University Press: New York, 1996.
(33) Roussel, F.; Buisine, J.-M *Phys. Rev. E* **2000**, *62*, 2310.

MA020726A